2011년 2월

석사학위 논문

# Fabrication of Explosives sensor Based on n-Type Porous Silicon by Controlling of an Etching Time and Applied Current Densities

조선대학교 대학원

화 학 과

조 보 민

# Fabrication of Explosives sensor Based on n-Type Porous Silicon by Controlling of an Etching Time and Applied Current Densities

식각시간 및 식각전류에 따른 n-Ptype 다공성 실리콘의
발광 특성을 기초로한 폭발물 센서로써의 제작

2011년 2월 25일

조 선 대 학 교 대 학 원

화 학 과

조 보 민

# Fabrication of Explosives sensor Based on n-Type Porous Silicon by Controlling of an Etching Time and Applied Current Densities

지도교수 손 홍 래

이 논문을 이학석사학위 논문으로 제출함.

2010년 10월

조선대학교 대학원

화 학 과

조 보 민

# 조보민의 석사학위논문을 인준함

위원장 조선대학교 조 성 동 교수 (인)

위　원 조선대학교 고 문 주 교수 (인)

위　원 조선대학교 손 홍 래 교수 (인)

2010년 11월

# 조선대학교 대학원

# LIST

## Chapter 2. Fabrication of Gradient Optical Filter Containing Anisotropic Bragg Nanostructure

Chapter 3. Porous Silicon Platform for Rapid Detection of Functionalized Superparamagnetic Beads via Magnetic Manipulation

# LIST OF TABLES



# LIST OF FIGURES

# 초 록

## 각시간 및 식각전류에 따른 n-Ptype 다공성 실리콘의 발광 특성을 기초로한 폭발물 센서로써의 제작

석사과정 : 조 보 민
지도교수 : 손 홍 래
조선대학교 화 학 과

다공성 실리콘은 1입방센티미터당 수백 평방미터에 해당하는매우 큰 특정한 표면적을 가지고, 이것은 순수실리콘 웨이퍼 표면적의 약 천배에 해당하여 기체나 액체센서로의 응용에 이상적이다. 저항값이 1-10Ωcm인 n-Type 실리콘웨이퍼를 일반적으로 HF와 에탄올 용매를 이용하여 전기화학적 식각을 수행하면 발광특성을 갖는 다공성 실리콘이 만들어진다. 이실험에서 발광특성을 갖는 다공성 실리콘은 galvanostat을 이용하여 정전류를 흘려주어 얻을 수 있다. 다공성 실리콘의 발광 특성과 표면의 형태는 식가신간과 전류밀도의 조절과밀접한 관계가 있다. 다공성 실리콘은 표면이 대부분 수소원자로 둘러싸여진 실리콘 나노결정의로 연결되어 존재한다. 본 연구에 사용된 다공성 실리콘 시료는 자외선 파장을 여기 파장으로 하였을 때 가시영역대에서 강한 붉은 발과 특성을 보인 것을 사용하였다.

붉은색의 발광 특성은 다공성 실리콘에서 실리콘 나노결정의 양자가둠표과에 기인한다 다공성 실리콘 샘플은 전류 밀도 50-700mA/$cm^2$ 까지의 범위에서 50-300초 동안 흘려줌으로 인해 준비하였다. 각각의 식각전류의 변화에 따른 발광 스펙트럼들을 나타낸 것이다. 50-300초의 식각시간으로 각각의 식각 전류로부터 얻은 다공성 실리콘의 발광 스펙트럼 식각 시간을 일정하게하고 식각전류의 세기를 변화시켰을 때 식각 전류의 세기가 200mA일 경우 가장 높은 발광 효

율을 얻었으며, 200mA 보다 높은 식각전류를 이용하여 전기화학적 식각을 하였을 때 다공성 실리콘의 발광세기는 감소하는 경향을 얻었다. 800mA 이상의 식각전류를 흘려주었을 경우에는 다공성 실리콘이 형성되지 않고 붕괴되어 필름이 실리콘 웨이퍼로부터 분리되어 식각 도중에 뜨는 현상이 발견되었다. 식각전류가 200mA 이하인 경우에도 역시 다공성 실리콘의 발광특성이 감소하는 현상을 얻었다.

# Chapter 1. Investigation of Photoluminescence Efficiency of n-Type Porous Silicon by Controlling of an Etching Time and Applied Current Densities

Cho, Bomin
Advisor : Prof. Sohn, Honglae, Ph.D,
Department of Chemistry,
Graduate School of Chosun University

## Abstract

Photoluminescence properties and surface morphologies of porous silicon were investigated by controlling of etching times and applied current densities. FE-SEM image of porous silicon surface indicated that the porous silicon prepared at currents below 200 $mA/cm^2$ exhibited very stable and even surface. However the porous silicon prepared at currents above 300 $mA/cm^2$ displayed the cracked surface of porous silicon. This cracked surface was collapsed to give cracked domains at currents over 500 $mA/cm^2$. Photoluminescence of porous silicon was investigated by controlling of etching times and applied current densities in the range from 50 sec. to 900 sec. and from 50 $mA/cm^2$ to 800 $mA/cm^2$, respectively. Photoluminescence intensity of porous silicon increased gradually during etching process, reached maximum, and then decreased as the etching time increased. Porous silicon showed the best photoluminescence efficiency was prepared at currents of 200 $mA/cm^2$ and etching time of 300 sec.

# Ⅰ. Introduction

Since the discovery of visible photo- and electroluminescence from nanocrystalline porous silicon[1,2], porous silicon has been intensively investigated for a variety of applications such as chemical[3] and biological sensors[4], medical diagnostics[5], optical band pass filters [6], micro chemical reactors[7], and micro fuel cells[8]. Porous Si is an ideal candidate for gas- or liquid- sensing applications, since it has a very large specific surface area on the order of few hundreds $m^2/cm^3$, corresponding to about thousand times of the surface area of a polished silicon wafer. Photoluminescence property has been exploited to develop porous silicon sensors for detection of toxic gases[9,10], solvents[11,12]. Luminescent porous silicon samples can be usually prepared by a galvanostatic photoetch of n-type silicon wafer. Till date, it is assumed that light emission most likely results from quantum confinement effects within silicon nanocrystallites and nanowires imbedded within the porous matrix. Room temperature, visible photoluminescence with an external quantum efficiency of up to 5% can be routinely achieved upon irradiation with UV or blue light[13]. Intensity of photoluminescence depends on the presence of surface adsorbates[14]. Organic vapors have been detected quantitatively by quenching of photoluminescence of the quantum-confined silicon crystallites in porous silicon[15-21]. In this work, photoluminescence properties and surface morphologies of porous silicon were investigated by controlling of etching times and applied current densities.

# Ⅱ. Experimental Section

## 2.1. Etching Set-up for Porous Silicon Surface

Heavily doped n-type silicon wafers (P-doped, orientation<100>, Siltronix, Inc.) with a resistivity in the range 1~10 Ω•cm were used to fabricate photoluminescence porous silicon by an anodic etch in ethanolic HF consisted of a 1:1 volume mixture of aqueous 48% hydrofluoric acid (Aldrich) and absolute ethanol (Aldrich). The galvanostatic etch was carried out in a Teflon cell by using a two-electrode configuration with a Pt mesh counter electrode. Porous silicon was prepared by using various etching times and applied current densities. The anodization current was supplied by a Keithley 2420 high-precision constant current source. Galvanostatic etching was performed under the illumination with a 300 W tungsten filament bulb for the duration of etch. All samples were then rinsed several times with ethanol and dried under argon atmosphere prior to use. After etching, the samples were rinsed with ethanol, dried under a stream of dry $N_2$(g),and then dried in vacuum for 30min priortouse.

## 2.2. Instrumentation and data acquisition

Steady-state photoluminescence spectra were obtained with an Ocean Optics S2000 spectrometer fitted with a fiber optic probe. The excitation source was a LED ($\lambda$max = 480 nm) focused on the sample (at a 450 angle to the normal of the surface) by means of a separate fiber. Light was collected at a 900 angle to the incident light source with a fiber optic. Spectra were recorded with a CCD-detector in the wavelength range of 400 to 900 nm. Values of percent quenching are reported as (I0-I)/I0, where I0 is the intensity of the luminescence of porous silicon, integrated between 400 and 900 nm, in

the absence of quencher and I is the integrated intensity of luminescence of porous silicon in the presence of a quencher. The surface morphology of porous silicon was observed with cold field emission scanning electron microscope (FE-SEM, S-4700, Hitachi).

## Ⅲ. Results and Discussion

### 3.1. Surface Characterization of Porous Silicon

An anodic etch of n-type silicon wafer with resistivities of 1~10 Ωocm in ethanolic HF solution generally produced photoluminescence porous silicon. In this work, photoluminescence porous silicon was been successfully fabricated by using a galvanostatic electrochemical etch. Photoluminescence properties and surface morphologies of porous silicon were investigated by controlling of etching times and applied current densities. Porous silicon consisted of a large number of interconnected Si nanocrystallites with a surface that is almost entirely covered with hydrogen atoms. Porous silicon samples prepared by a galvanostatic photoetch of silicon wafer in this study exhibited a strong visible red photoluminescence possibly due to the photoetch. The red photoluminescence is due to the quantum confinement of silicon nanocrystallites in porous silicon. Porous silicon samples were prepared by using applied current densities in the range from 50 to 700 $mA/cm^2$ of and 300 sec. of etching times. Surface morphologies were obtained with cold FE-SEM and shown in Fig. 1. FE-SEM image of porous silicon surface indicated that the porous silicon prepared at currents below 200 $mA/cm^2$ exhibited very stable and even surface. However the porous silicon prepared at currents above 300 $mA/cm^2$ displayed the cracked surface of porous silicon. This cracked surface was collapsed to give cracked domains at currents over 500 $mA/cm^2$.

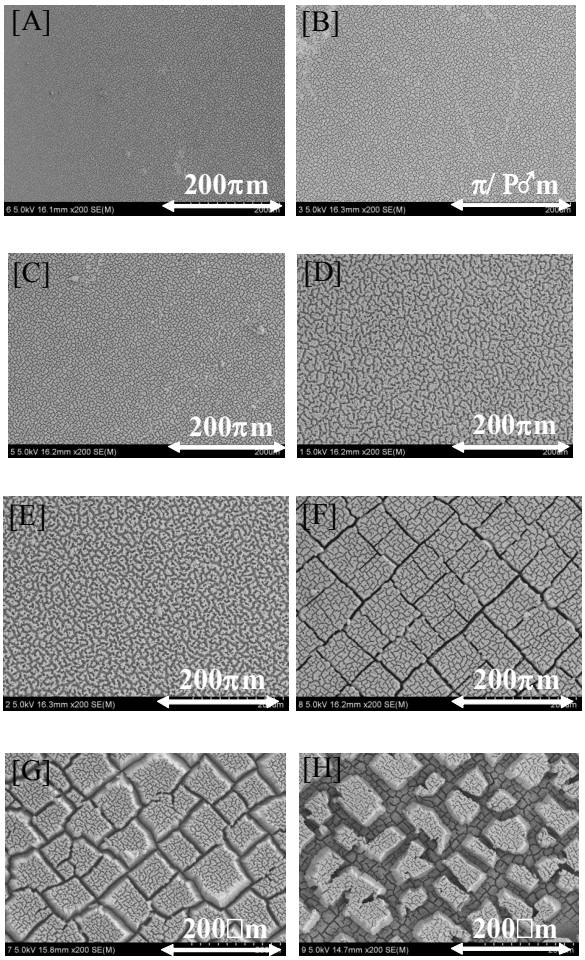


Fig. 1. Surface SEM images of photoluminescence porous silicon prepared at current densities of 50 mA/cm$^2$(A), 100 mA/cm$^2$(B), 200 mA/cm$^2$(C), 300 mA/cm$^2$(D), 400 mA/cm$^2$(E), 500 mA/cm$^2$(F), 600 mA/cm$^2$(G), and 700 mA/cm$^2$(H)

### 3.2. Photoluminescence Properties of Porous Silicon

Photoluminescence spectra were measured at room temperature and the emission spectra were collected with 480 nm of excitation wavelengths. Porous silicon samples were prepared by using etching

times in the range from 400 to 900 sec. at fixed applied current densities (100 mA/cm2). Fig. 2 showed the steady-state photoluminescence spectra of porous silicon samples and indicated that the maximum intensity of emission spectrum was centered at 645 nm with an excitation wavelength of 480 nm. Photoluminescence intensity of porous silicon increased gradually during etching process, reached maximum in 800 sec, and then decreased as the etching time increased. An emission wavelength of 645 nm shifted slightly to the shorter wavelength by 15 nm as the etching time increased.

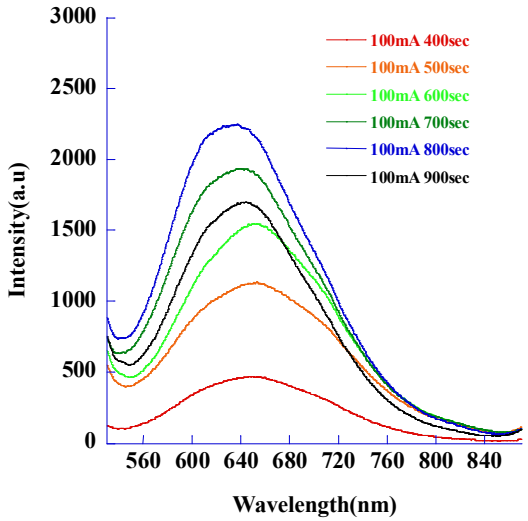


**Fig. 2.** Photoluminescence spectra of porous silicon prepared at 100 mA/cm$^2$ of current densities with various etching time (from top, 800, 700, 900, 600, 500, 400 sec.).

Photoluminescence of porous silicon was investigated by controlling of etching times and applied current densities in the range from 50 sec. to 900 sec. and from 50 mA/cm$^2$ to 800 mA/cm$^2$, respectively. Table 1 summarized the photoluminescence intensities of porous

silicon samples prepared by above conditions. In case of 50 and 100 mA/cm$^2$, the photoluminescence of porous silicon appeared after 400 sec of etching time. Photoluminescence of porous silicon prepared at currents of 200, 300, and 400 mA/cm$^2$ appeared after 100 sec of etching time. Photoluminescence of porous silicon prepared at currents above 500 mA/cm$^2$ appeared right after etching of silicon wafer.

| B \ A | 50 | 100 | 200 | 300 | 400 | 500 | 600 | 700 | 800 |
|---|---|---|---|---|---|---|---|---|---|
| 50 | - | - | - | - | - | 179 | 219 | 162 | 188 |
| 100 | - | - | 539 | 956 | 358 | 320 | 564 | 135 | 726 |
| 200 | - | - | 1982 | 2606 | 2435 | 2636 | 2230 | 2337 | 1291 |
| 300 | - | - | 3915 | 1981 | 1802 | 1290 | 925 | 752 | 230 |
| 400 | 665 | 467 | 2803 | 1391 | 204 | 223 | 230 | 202 | - |
| 500 | 1615 | 1133 | 2811 | 476 | - | - | - | - | - |
| 600 | 1748 | 1135 | 2346 | - | - | - | - | - | - |
| 700 | 1929 | 1935 | 823 | - | - | - | - | - | - |
| 800 | 928 | 2239 | 479 | - | - | - | - | - | - |
| 900 | 878 | 1697 | - | - | - | - | - | - | - |

Table 1. Summary of photoluminescence intensities of porous silicon prepared from different etching parameters (A=current, mA/cm$^2$, B=time, sec.).

Fig. 3 illustrated how the photoluminescence efficiency of porous silicon might be changed during the etching procedure. Photoluminescence efficiency of porous silicon increased as the etching time increased, reached to the maximum efficiency, and then decreased with further etching time. Porous silicon showed the best photoluminescence efficiency was prepared at currents of 200 mA/cm$^2$ and etching time of 300 sec.

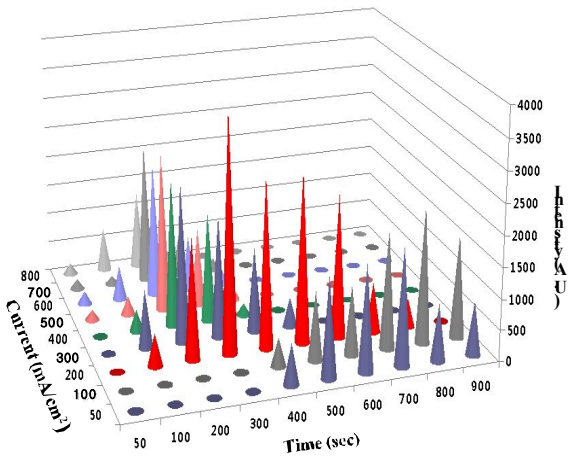


Fig. 4. Comparison of photoluminescence intensities of porous silicon prepared from different etching parameters

## IV. Conclusion

Surface morphology of porous silicon prepared at currents below 200 $mA/cm^2$ exhibited very stable. However the porous silicon prepared at currents above 300 $mA/cm^2$ displayed the cracked surface and then collapsed to cracked domains. Photoluminescence of porous silicon was investigated at various etching times and applied current densities. As etching time increased, the photoluminescence efficiency of porous silicon prepared increased. However, this photoluminescence efficiency start to decrease, after it reached to maximum

## Ⅴ. References

[1] L. T. Canham, Appl.Phys.Lett.57, 1046 (1990).

[2] K. D. Hirschman, L. Tsybeskov, S. P. Duttagupta, and P. M. Fauchet, Nature 384, 338 (1996).

[3] H. Sohn, S. Letant, M. J. Sailor, and W. C. Trogler, J. Am. Chem. Soc. 122, 5399 (2000).

[4] V. S. Lin, K. Motesharei, K. S. Dancil, M. J. Sailor, and M. R. Ghadiri, Science 278, 840 (1997).

[5] M. Simion, I. Kleps, T. Neghina, A. Angelescu, M. Miu, A. Bragaru, M. Danila, E. Condac, M. Costache, and L. Savu, J. Alloy. Compd. 434, 830 (2007).

[6] S. Ilyas, T. B?cking, K. Kilian, P. J. Reece, J. Gooding, K. Gaus, and M. Gal, Opt. Mater. 29, 619 (2007).

[7] M. A. Khan, M. S. Haque, H. A. Naseem, W. D. Brown, and A. P. Malshe, Thin Solid Films 332, 93 (1998).

[8] S. E. L?tant, S. Content, T. T. Tan, F. Zenhausern, and M. J. Sailor, Sensor Actuat. B- Chem. 69, 193 (2000).

[9] S. Jang, J. Kim, Y. Koh, Y. C. Ko, H. -G. Woo, and H. Sohn, J. Nanosci. Nanotechnol. 7, 4049 (2007).

[10] S. Jang, Y. Koh, J. Kim, J. Park, C. Park, S. J. Kim, S. Cho, Y. C. Ko and H. Sohn, Mater. Lett. 62, 552 (2008).

[11] P. A. Snow, E. K. Squire, P. S. J. Russell, and L. T. Canham, J. Appl. Phys. 86, 1781 (1999).

[12] S. G. Kim, S. Kim, Y. C. Ko, S. Cho, H. Sohn, Colloids Surf. A: Physicochem. Eng. Aspects 313, 398 (2008).

[13] G. Cullins, L. T. Canham, P. D. J. Calcott, J.Appl.Phys.82 ,909 (1997).

[14] J. H. Song, M. J. Sailor, J. Am. Chem. Soc. 119, 7381 (1997).

[15] S. Content, W. C. Trogler, M. J. Sailor,Chem.Eur.J. 6, 2205 (2000).

[16] G. Cullis, L. T. Canham, P. D. J. Calcott, J. Appl. Phys. 82, 909 (1997).

[17] M. Ben-Chorin, A. Kux, and I. Schechter, Appl. Phys. Lett. 64, 481 (1993).

[18] J. L. Coffer, S. C. Lilley, R. A. Martin, and L. A. Files-Sesler, J. Appl. Phys. 74, 2094 (1993).

[19] J. Harper, M. J. Sailor, Anal. Chem. 68, 3713 (1996).

[20] J. H. Song, M. J. Sailor, J. Am. Chem. Soc. 119, 7381 (1997).

[21] D.-A. Kim, J.-H. Shim, N.-H. Cho, Appl. Surf. Sci. 234, 256 (2004).

# Chapter 2. Fabrication of Gradient Optical Filter Containing Anisotropic Bragg Nanostructure

Cho, Bomin
Advisor : Prof. Sohn, Honglae, Ph.D,
Department of Chemistry,
Graduate School of Chosun University

## Abstract

New gradient optical filters containing asymmetric Bragg structure were prepared from the distributed Bragg reflector (DBR) porous silicon (PSi). Anisotropic DBR PSi displaying a rainbow-colored reflection was generated by using an asymmetric etching configuration. Flexible anisotropic DBR PSi composite films were obtained by casting of polymer solution onto anisotropic DBR PSi thin films. The surface and cross-sectional images images of anisotropic DBR PSi composite films obtained with cold field emission scanning electron microscope indicated that the average pore size and the thickness of porous layer decreased as the lateral distance increased. As lateral distance increased, the reflection resonance shifted to shorter wavelength.

# Ⅰ. Introduction

The development of photonic materials represents one of the interesting challenges in modern materials science. The photonic crystal/polymer composites materials are particularly attractive due to the combined advantages of unique optical properties, and flexible possibilities. PSi is an attractive candidate for building photonic structure, because the porosity and average pore size can be tuned by adjusting the electrochemical preparation conditions that allow the construction of photonic crystals.[1] PSi has been investigated for a variety of applications such as chemical and biological sensors,[2,3] medical diagnostics,[4] optical band pass filters,[5] micro chemical reactors,[6] and micro fuel cells.[7] Its importance is due to very high surface area as well as their unique photonic properties. In recent years, optical devices based on multi-structured PSi, both DBR and rugate PSi[8,9] providing a reflection band at a desired wavelength in the optical reflectivity spectrum are actively exploited due to their high reflectivity. DBR-structured PSi having the photonic structure of a Bragg filter can be generated by applying a computer-generated square current density. However PSi is limited by their chemical and mechanical stability for many applications, because these films are very brittle.[10] To eliminate these issues, PSi composite material would be ideal. Here we prepared a flexible anisotropic DBR PSi/polymer composite film displaying a rainbow colored reflection for possible applications as tunable band-rejection.

# Ⅱ. Experimental Section

## 2.1. Preparation of Anisotropic DBR PSi Samples

Anisotropic DBR PSi sample was prepared by an electrochemical etching of the heavily doped p-type Si <100> substrate (boron doped, polished on the (100) face, resistivity of 0.8-1.2 mΩocm, Siltronix, Inc.). The etching solution consists of a 1:3 by volume mixture of absolute ethanol (ACS reagent, Aldrich Chemicals) and aqueous 48% HF (ACS reagent, Aldrich Chemicals). Etching was carried out in a Teflon cell by using a two-electrode configuration with a Pt plate counter electrode placed at the end of etching cell to have the structural anisotropies. Anisotropic DBR PSi sample was prepared by using a computer-generated periodic square wave current density between 320 $mA \cdot cm^{-2}$ for 1.2 s and 100 $mA \cdot cm^{-2}$ for 7.2 s with 50 repeats of 420 s. To prevent the photo-generation of carriers, the anodization was performed in the dark. All samples were then rinsed several times with ethanol and dried under argon atmosphere prior to use.

## 2.2. Preparation of Anisotropic DBR PSi Composite Films

Free-standing anisotropic DBR PSi films were obtained from the silicon substrate by an applying of electropolishing current at 300 $mA \cdot cm^{-2}$ for 1 min in an ethanoic 37.5% aqueous HF solution, and then at 8 $mA \cdot cm^{-2}$ for 5 min in ethanoic 3.3 % aqueous HF solution. Free-standing anisotropic DBR PSi films were thermally oxidized in the furnace at 300℃ for 3 hrs. For the anisotropic BDR composite films, 3 g of polystyrene (Aldrich, Mw = 280,000) were dissolved in 20 mL of toluene (Fisher Scientific). The polymer solutions were cast onto the anisotropic DBR PSi films and the samples were annealed in an oven at 50℃ for 3 hr.

### 2.3. Instruments and Data Acquisitions

The anodization current was supplied by a Keithley 2420 high-precision current source which is controlled by a computer to allow the formation of anisotropic DBR PSi films. Interferometric reflectance spectra of anisotropic DBR PSi were recorded by using an Ocean Optics S2000 spectrometer fitted with a bifurcated fiber optic probe. A tungsten-halogen light source was focused onto the spot of anisotropic DBR PSi composite films. Spectra were recorded with a CCD detector in the wavelength rang 400~1200 nm. The illumination of the surface as well as the detection of the reflected light was performed along an axis coincident with the surface normal. FT-IR instrument in the diffuse reflectance mode (Spectra-Tech diffuse reflectance attachment), with diffuse reflectance absorption spectra are reported in absorbance units. The morphology of anisotropic DBR PSi composite film was observed with cold field emission scanning electron microscope (FE-SEM, S-4700, Hitachi).

## Ⅲ. Results and Discussion

Since the discovery of DBR PSi from silicon wafer, research has been associated with emerging technologies, such as photonic crystals for optical band pass filters. DBR PSi is an attractive candidate for building nanostructured composite materials because the porosity and average pore size can be tuned by adjusting the electrochemical preparation conditions that allow the construction of photonic crystals. DBR PSi exhibits a high reflectivity band with a Bragg wavelength, $\lambda_{Bragg}$, depending on the thickness of the layers ($d_1$, $d_2$) and the corresponding refractive indices ($n_1$, $n_2$). The mth order of the Bragg peak is given by

$$m\lambda_{Bragg} = 2(d_1n_1 + d_2n_2).$$

DBR PSi is typically prepared by an applying a computer generated periodic square-wave current between low and high current densities to the etch cell which results two distinct indices and exhibits a photonic structure of Bragg filter. In this work, anisotropic DBR PSi displaying a rainbow-colored reflection was generated by an electrochemical etching of silicon wafer with an asymmetric etching configuration as shown in Figure 5.

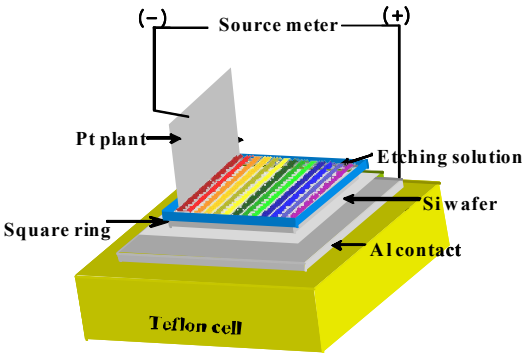


Fig. 5. Schematic diagram of the etch cell with plate Pt electrode for the formation of anisotropic DBR PSi.

Surface and cross-sectional SEM images of anisotropic DBR PSi were obtained by using a cold field emission scanning electron microscope as shown in Figure 6. The surface SEM images of anisotropic DBR PSi indicated that the average pore size decreased as the lateral distance (x) from the Pt counter electrode increased. The cross-sectional SEM images of anisotropic DBR PSi indicated that the anisotropic DBR PSi had a depth of several decade microns. A repeating etching process resulted in two distinct refractive indices. The thickness of anisotropic DBR PSi layer also decreased as the lateral distance increased.

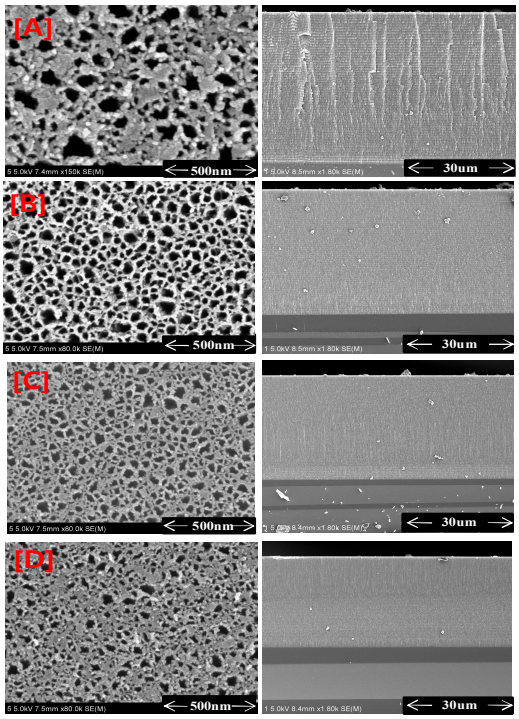


Fig. 6. Surface (left) and cross-section (right) images of anisotropic DBR PSi measured at the lateral distance from a point closest to the Pt counter electrode to the silicon surface: [A] at 0 mm, [B] at 30 mm, [C] at 45 mm, and [D] at 60 mm.

After the generation of anisotropic DBR PSi, free-standing anisotropic DBR PSi film was lifted off from the silicon substrate by an applying of electropolishing current and thermally oxidized in the furnace. For the anisotropic BDR composite films, polystyrene solution dissolved in toluene were cast onto the anisotropic DBR PSi films and annealed in an oven. Schematic diagram and photographs for the generation of anisotropic DBR PSi composite film were shown in Figure 6.

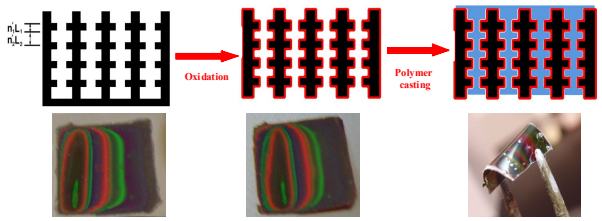


Fig. 7. Schematic diagram for the generation of anisotropic DBR PSi composite film and photographs of free-standing anisotropic DBR PSi film (left), oxidized anisotropic DBR PSi film (middle), and anisotropic DBR PSi composite film (right).

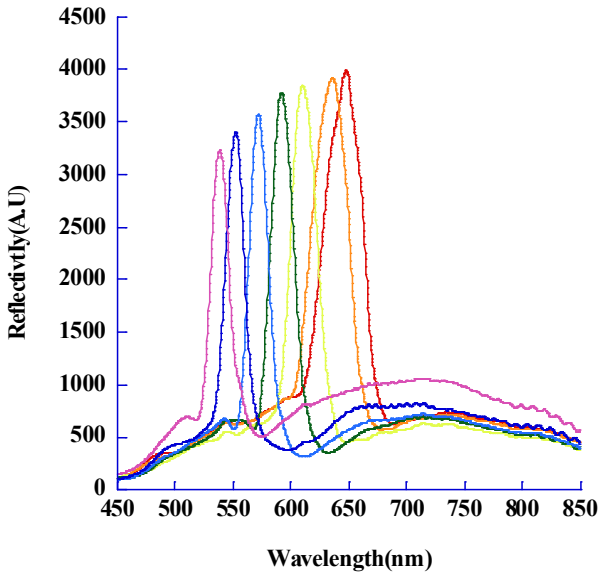


Fig. 8. Reflection spectra of anisotropic DBR PSi composite film as a function of lateral distance displayed reflection maxima of 650, 632, 612, 590, 574, 551, 534 nm at lateral of 0, 15, 30, 45, 60, 75, 90 mm, respectively.

The reflection spectra of anisotropic DBR PSi composite film were

shown in Figure 8. The reflection resonances were measured as a function of lateral distance from a point closest to the plate Pt counter electrode to a position on the silicon surface. A tungsten light source was focused onto the surface of anisotropic DBR PSi composite film with a spot size of approximately 1 - 2 mm. Increase of lateral distance caused the decrease of porous silicon depth and the reflection resonance to shift to shorter wavelength. The plot for the relationship between the reflection wavelength maximum and the distance from the Pt electrode shown in Figure 9 exhibited a linear profile.

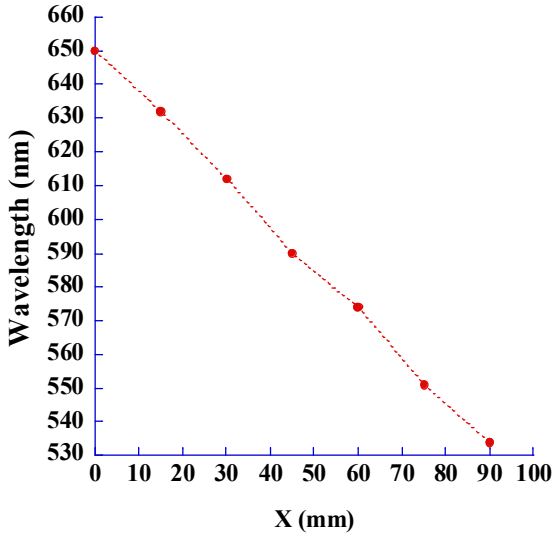


Fig. 9. Reflection wavelength maximum as a function of distance on the anisotropic DBR PSi composite film.

## Ⅳ. Conclusion

Flexible anisotropic DBR PSi composite film showing a rainbow-colored reflection was successfully fabricated by using an asymmetric etching configuration. The surface and cross-sectional images image of anisotropic DBR PSi indicated that the average pore size and the thickness of porous layer decreased as the lateral distance increased. As lateral distance increased, the reflection resonance shifted to shorter wavelength with linear relationship.

## Ⅴ. References

[1]. F. Cunin, T. A. Schmedake, J. R. Link, Y. Y. Li, J. Koh, S. N. Bhatia, and M. J. Sailor, Nat. Mater. 1, 39 (2002).

[2]. H. Sohn, S. Letant, M. J. Sailor, and C. Trogler, J. Am. Chem. Soc. 122, 5399 (2000).

[3]. V. S. Lin, K. Motesharei, K. S. Dancil, M. J. Sailor, and M. R. Ghadiri, Science 278, 840 (1997).

[4]. E. J. Anglin, L. Cheng, W. R. Freeman, and M. J. Sailor, Adv. Drug Deliver. Rev. 60, 1266 (2008).

[5]. J. Kim, S. Jang, Y. Koh, C. Park, H.-G. Woo, S. Kim, and H. Sohn, J. Nanosci. Nanotechnol. 8, 4951 (2008).

[6]. J. L. Gole, J. Corno, S. Ozdemir, S Prokes, and H.-C. Shin, Phys. Status. Solidi. 5, 1773 (2009).

[7]. S. Desplobain, G.. Gautier, L. Ventura, and P. Bouillon, Shin, Phys. Status. Solidi. A 206, 1282 (2009).

[8]. J. Kim, Y. Koh, S. Jang, Y.C. Ko, H.-G. Woo, and H. Sohn, J. Nanosci. Nanotechnol. 7, 4165 (2007).

[9]. A.M. Ruminski, B.H. King, J. Salonen, J.L. Snyder, and M.J. Sailor, Adv. Funct. Mater. 20, 2874 (2010).

[10]. M. Ghulinyan, C. J. Oton, G. Bonetti, Z. Gab urro, and L. Pavesi, J. Appl. Phys. 93, 9724 (2003).

# Chapter 3. Porous Silicon Platform for Rapid Detection of Functionalized Superparamagnetic Beads via Magnetic Manipulation

Cho, Bomin
Advisor : Prof. Sohn, Honglae, Ph.D,
Department of Chemistry,
Graduate School of Chosun University

## Abstract

Biosensing technology offering an inexpensive, sensitive, and portable means of detecting trace amounts of target analytes is an important area of research. The unique properties of porous silicon (PSi) is considered to an important component for the realization of such technology. Here we demonstrate a rapid and highly sensitive method for detecting magnetic nanoparticle labels for biosensing using nano-structured PSi. The time for chemical bonding between target chemical and functionalized magnetic labels was reduced using an external magnetic field, and bonding detected by monitoring changes of the intensity of reflected light scattered from nanoparticles attached on surface of PSi. The optical change was proportional to the number of magnetic beads and size of beads on the PSi surface.

## Ⅰ. Introduction

A wide range of sensing methods based on porous silicon (PSi) has been reported for monitoring chemical analytes and biomedical diagnostics.[1-3] The PSi-based biosensing platform shows potential as a biosensing technology for point of care treatment (POCT) because of the small size and versatility of this approach. In addition to downsizing, PSi also has unique optical properties such as interferometric phenomenon and photonic crystal effects.[4-5] Such optical properties are tunable by the appropriate design of the diameter of pores and homogenous porosity. Despite these advantages of PSi over other optical methods.[1-5], PSi-based biosensing protocol requires long durations of time for biomolecules to diffuse deep inside pore walls for complementary binding. Now, there have been many reports on the use of 'magnetic-labels SPBs (superparamagnetic beads with biomolecules comparable size in actual biomolecules), enabling the shortening of the time taken for the physical chemical reaction by the use of external magnetic fields.[6-8] Typically, magnetic beads are used for molecular separation where an external magnetic field enables the rapid collection of biomolecuels of interest in a solution9). In this work, we propose a new biosensing method based on monitoring changes in the intensity of reflected light due to chemical binding of SPBs by functionalized PSi surfaces. The speed of the chemical reaction was enhanced by the use of an external magnetic field to collect carboxyl-terminated SPBs onto the amine-terminated surface of PSi. Changes in the intensity of the optical reflection depended on the areal concentration of magnetic beads attached onto the PSi surfaces, where larger concentrations of magnetic beads resulted in higher changes in the intensity of

reflected light. Our protocol based on monitoring changes in the intensity of reflected light is a promising means for the detection of small amounts of biomolecules in a short period of time.

## Ⅱ. Experimental Section

One method to introduce layers of periodic optical nanostructures into silicon wafers is by electrochemical anodization in hydrogen fluoride (HF) solution10-11). The silicon wafers used in this study were heavily doped p++-type (boron doped, polished on the <100> face, resistivity of 0.8-1.2mΩ cm, Siltronix Inc.). The solution used for electrochemical anodization composited of a 3:1 volume mixture of aqueous 48% HF solution and pure ethanol. Periodic structures of PSi were achieved by the use of periodic square wave current densities. Our samples were prepared by utilizing periodic square wave current densities: 50 $mAcm^{-2}$ for 3 s and 5 $mAcm^{-2}$ for 90 s with 20 repetitions. Subsequently, the substrates were rinsed in pure ethanol and dried under argon atmosphere.The detection of chemical affinity was conducted as follows: First, the PSi samples were treated in an oxygen plasma resulting in the oxidization of the surface of the samples, followed by the immobilization of amino group (NH2) on the surface of PSi using an amino-functional silane [3-propyltrimethoxysilane (APTS)] as an adhesive. Next, the amine-terminated substrates were placed under a light source, and a colloidal solution consisting of a phosphate buffer solution (PBS: pH 7.0) and carboxyl-terminated nanometer sized SPBs was dropped onto the substrate. Subsequently, a NdFeB magnet was placed underneath the substrate to apply a magnetic field perpendicular to the plane of the surface. The magnetic field attracted and collected the SPBs rapidly onto the surface of the PSi, resulting in a drastic reduction of the time required for the amide reaction between the PSi surface and SPBs. Finally, we monitored the changes in the intensity of reflected light with time. For the data acquisition, the samples were illuminated with a tungsten lamp, and the reflected light spectrum was measured using an Ocean Optics 4000 spectrometer integrated into optical fibers.

## Ⅲ. Results and Discussion

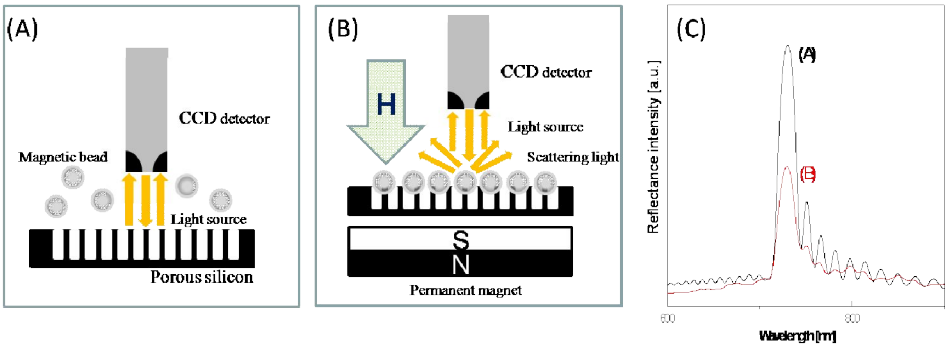


**Fig. 10.** A schematic of an experimental setup for the detection of magnetic beads on porous silicon (PSi) substrate; (A) Immediately after dropping the colloidal solution onto the substrates in absence of the external magnetic field; (B) Collection of SPBs onto the surface of PSi in application of the external magnetic field gradient; (C) Changes in the intensity of reflected light due to the presence of SPBs on the surface of PSi.

Fig.10 is a schematic of our method for the detection of functionalized-SPBs. Immediately after dropping the colloidal solution onto the substrates, incident light was incident onto the surface of PSi and was reflected back to the CCD detector without any interruption caused by dispersed nanometer sized magnetic beads as shown in Figure 10(A). The spectrum of the reflected light intensity corresponds to the black line in Fig. 10 (C). When an external magnetic field was applied, the SPBs were magnetized and collected at the PSi surface. Notably, SPBs with sizes larger than the pores of the samples were rapidly collected onto the surface of PSi, not going deep inside the pores. The pores were covered with clusters of

nanometer sized SPBs as depicted in Fig. 10(B). The incident light undergoes additional scattering, leading to a difference reflectance spectrum. The incident light was most likely scattered by the SPBs blocking the PSi pores. Importantly, the intensity of reflected light corresponding to the red line in Fig.10 (C) was distinguishable from the measured light intensity when there were no SPBs on the surface of the PSi.

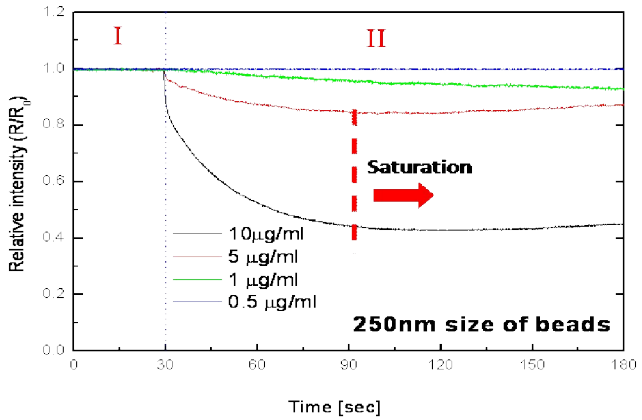


**Fig. 11.** The R/R0 is defined as the ratio of the intensity of reflected light after application of the external magnetic field with time to that at t = 0, immediately after dropping the colloidal solution containing 250-nm-diameter SPBs. Region I : Absence of the magnetic field. Region II :Application of a magnetic field (500 Oe).

Fig. 11 shows the results of the reflectance as function of time for different concentrations of the 250 nm size of magnetic beads. At time t = 0 s, the colloidal solution containing 250-nm-diameter SPBs was dropped on the PSi substrate, yielding a stable optical signal. At 30 sec, the magnetic field was applied to start collecting SPBs onto the surface of the PSi, resulting in the decrease in the

intensity of reflected light with time. The intensity of reflected light stopped decreasing in less than 60 sec after application of the external magnetic field. Colloidal solutions with a higher concentration of SPBs showed greater changes in the intensity of reflected light. It is thought that the large numbers of carboxyl-terminated SPBs reacting with amine group immobilized on the surface of the PSi were attached on the PSi surface, resulting in blocking and scattering the incident light. More importantly, the chemical reaction was dramatically enhanced by the use of the external magnetic field (less than 60 sec).

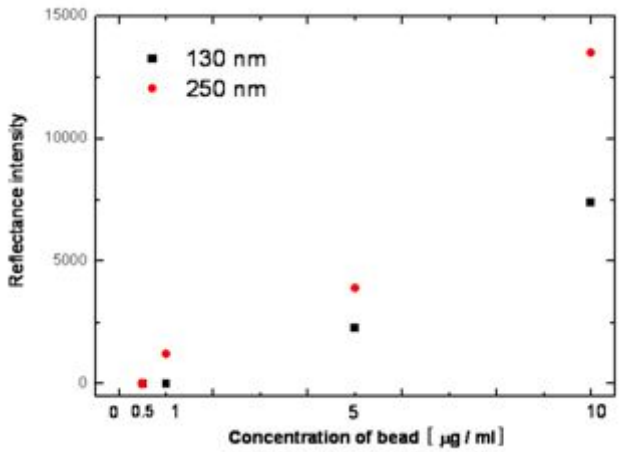


Fig. 12. The intensity of reflected light as a function of the concentration of SPBs (130 nm, 250 nm) in colloidal solution.

The relationship between intensity of the reflected light and concentration of carboxyl-terminated SPBs in the colloidal solution was studied after sensing with the application of a magnetic field (Fig. 12). Our detection method enabled the detection of SPBs with concentrations as small as 1 μg/ml. As describe above, the change in the intensity of reflected light was greatly affected by the

concentration of SPBs on the surface.

The intensity change of the reflected light is explained by the Mie theory, especially Mie total cross section calculation.12) The Mie total cross section consists of total scattering, absorption and extinction, denoted as σsc, σab and σex, respectively. The total scattering cross section is defined as the ratio of the total radiant power scattered by a particle in all directions to the radiant power incident on the particle. The general expression of Mie total scattering cross is given by 13-14)

$$\sigma_{sc} = \left(\frac{2}{x^2}\right)\sum_{n=1}^{\infty}(2n+1)(|a_n|^2 + |b_n|^2),$$

where, x = 2πR / λ. (where R is the radius of the particle and λ is the wavelength of incoming radiation). an and bn are Mie scattering coefficients.

The Mie total scattering cross section, efficiency factors of scattering were coefficients (an and bn) 13-14) that determine the scattering characteristics of a particle or a particulate medium. These functions were obtained from information of the scattering conditions (i.e. particle size, particle refractive index, and light wavelength). Therefore, the intensity of reflected light by the magnetic beads on PSi surface is inversely proportional the size and concentration of SPBs. Furthermore, the changes in the peak of the optical reflection were proportional to the areal density of magnetic beads attached to PSi surfaces. From changes of decrease in the light intensity we can detect probe-target binding of amide reactions.

## Ⅳ. Conclusion

We demonstrated a method for the rapid detect of chemical affinity by monitoring changes in the intensity of reflected light from SPBs attached on the surface of PSi. The reaction speed of chemical binding was greatly reduced by using the external magnetic field to collect the carboxyl-terminated SPBs onto the amine-terminated PSi surface. The change in the intensity of reflected light depended on to the areal concentrations of SPBs attached to PSi surfaces, where larger concentrations of SPBs on the surface resulted in great intensity decrease. By monitoring the change in the light intensity the chemical biding was easily detected less than 60 sec. Our method has potential used for the real biosensing.

## Ⅴ. References


[1]. K. A. Kilian, L. M. H. Lai, A. Magenau, S. Cartland, T. Bocking, N. Di Girolamo, M. Gal, K. Gaus, and J. J. Gooding: Nono Lett. 9 , 2021 (2009).

[2]. H. Sohn, S. Letant, M. J. Sailor, and W. C. Trogler: J. Am. Chem. Soc. 122, 5399 (2000).

[3]. V. S.-Y. Lin, K. Motesharei, K.-P. S. Dancil, M. J. Sailor, and M. R. Ghadiri: Science 278, 840 (1997).

[4]. S.M. Weiss, P.M. Fauchet: IEEE J. Sel. Top. Quantum Electron. 12 ,1514 (2006).

[5].T. Bo¨cking, K. A. Kilian, and K. Gaus: AdV. Funct. Mater. 18 3735 (2008).

[6]. A. Sandhu, Nature Nanotechnol. 2, 746 (2007).

[7]. Y. Morimoto, M. Abe, M. Hatakayama, H. Handa, and A. Sandhu: IEEE. Trans. Mag. 45, 2871 (2009).

[8]. Y. Morimoto, T. Takamura, S. Y. Park, S. Sakamoto, S. Kawata, H. Handa, and A. Sandhu: Jpn. J. Appl. Phys.49, 04DL07 (2010).

[9]. T. Ito, H. Ando, T. Suzuki, T. Ogura, K. Hotta, Y. Imamura, Y. Yamaguchi, H. Handa: science 327, 1345 (2010).

[10]. J. R. Link , and M. J. Sailor: PNAS 100, 10607 (2003).

[11]. Y. koh, S. Jang, J. Kim, S. Kim, Y. C. Ko, S. Cho, and H. Sohn: Colloids and Surfaces A: Physicochem. Eng. Aspects 313, 328 (2008).

[12]. C. Bohren, and D. Huffmann: Absorption and scattering of light by small particles; John Wiley & Sons: New York, (1983).

[13]. K Louedec, S Dagoret-Campagne and M Urban: Phys. Scr. 80, 035403 (2009).

[14]. A. J. Cox, Alan J. DeWeerd, and Jennifer Linden: Am. J. Phys. 70, 620 (2002).

# 저작물 이용 허락서

| 학 과 | 화학과 | 학 번 | 20097030 | 과 정 | 석 사 |
|---|---|---|---|---|---|
| 성 명 | 한글 : 조 보 민 한문 : 朝 甫 旼 영문 : Bomin Cho | | | | |
| 주 소 | 광주 광역시 북구 매곡동 서광인텔파크 106동 804호 | | | | |
| 연락처 | E-MAIL : chobomin2@hanmail.net | | | | |
| 논문 제목 | 한글 : 식각시간 및 식각전류에 따른 n-Type 다공성 실리콘의 발광 특성을 기초로한 폭발물 센서 제작<br>영문 : Fabrication of Explosives sensor Based on n-Type Porous Silicon by Controlling of an Etching Time and Applied Current Densities | | | | |

본인이 저작한 위의 저작물에 대하여 다음과 같은 조건아래 조선대학교가 저작물을 이용할 수 있도록 허락하고 동의합니다.

- 다 음 -

1. 저작물의 DB구축 및 인터넷을 포함한 정보통신망에의 공개를 위한 저작물의 복제, 기억장치에의 저장, 전송 등을 허락함
2. 위의 목적을 위하여 필요한 범위 내에서의 편집·형식상의 변경을 허락함. 다만, 저작물의 내용변경은 금지함.
3. 배포·전송된 저작물의 영리적 목적을 위한 복제, 저장, 전송 등은 금지함.
4. 저작물에 대한 이용기간은 5년으로 하고, 기간종료 3개월 이내에 별도의 의사표시가 없을 경우에는 저작물의 이용기간을 계속 연장함.
5. 해당 저작물의 저작권을 타인에게 양도하거나 또는 출판을 허락을 하였을 경우에는 1개월 이내에 대학에 이를 통보함.
6. 조선대학교는 저작물의 이용허락 이후 해당 저작물로 인하여 발생하는 타인에 의한 권리 침해에 대하여 일체의 법적 책임을 지지 않음
7. 소속대학의 협정기관에 저작물의 제공 및 인터넷 등 정보통신망을 이용한 저작물의 전송·출력을 허락함.

**동의여부 : 동의( ○ ) 반대( )**

2011년 2월

저작자: 조 보 민 (인)

# 조선대학교 총장 귀하